

The influence of large-scale magnetic field in the structure of supercritical accretion flow with outflow

Maryam Ghasemnezhad^{1★} and Shahram Abbassi^{2,3★}

¹Faculty of Physics, Shahid Bahonar University of Kerman, Kerman, Iran

²Department of Physics, School of Sciences, Ferdowsi University of Mashhad, 91775-1436 Mashhad, Iran

³School of Astronomy, Institute for Studies in Theoretical Physics and Mathematics, 19395-5531 Tehran, Iran

Accepted 2017 April 30. Received 2017 April 30; in original form 2017 April 9

ABSTRACT

We present the effects of ordered large-scale magnetic field on the structure of supercritical accretion flow in the presence of an outflow. In the cylindrical coordinates (r, φ, z) , we write the 1.5-dimensional, steady-state ($\frac{\partial}{\partial t} = 0$) and axisymmetric ($\frac{\partial}{\partial \varphi} = 0$) inflow–outflow equations by using self-similar solutions. Also, a model for radiation pressure supported accretion flow threaded by both toroidal and vertical components of magnetic field has been formulated. For studying the outflows, we adopt a radius-dependent mass accretion rate as $\dot{M} = \dot{M}_{\text{out}} \left(\frac{r}{r_{\text{out}}}\right)^{s+\frac{1}{2}}$ with $s = \frac{1}{2}$. Also, by following the previous works, we have considered the interchange of mass, radial and angular momentum and the energy between inflow and outflow. We have found numerically that two components of magnetic field have the opposite effects on the thickness of the disc and similar effects on the radial and angular velocities of the flow. We have found that the existence of the toroidal component of magnetic field will lead to an increase in the radial and azimuthal velocities as well as the relative thickness of the disc. Moreover, in a magnetized flow, the thickness of the disc decreases with increase in the vertical component of magnetic field. The solutions indicated that the mass inflow rate and the specific energy of outflow strongly affect the advection parameter. We have shown that by increasing the two components of magnetic field, the temperature of the accretion flow decreases significantly. On the other hand, we have shown that the bolometric luminosity of the slim discs for high values of \dot{m} ($\dot{m} \gg 1$) is not sensitive to mass accretion rate and is kept constant ($L \approx 10L_E$).

Key words: accretion, accretion discs – black hole physics – magnetic fields.

1 INTRODUCTION

The study of processes of gas accretion into compact objects started in the 1960s. The standard model, the supercritical accretion model and the radiatively inefficient accretion flow model are three models of accretion flow that have successfully explained energetic phenomena, including active galactic nuclei, ultraluminous X-ray sources and gamma-ray bursts. The optically thick super Eddington accretion flows (hereafter called slim discs) belong to the class of cold accretion flows. These flows proposed by Begelman & Meier (1982) and also Abramowicz et al. (1988) could describe the cold accretion flow structure in the ultraluminous X-ray sources and narrow-line Seyfert galaxies that cannot be explained by the tradi-

tional standard thin disc (Mineshige et al. 2000; Watarai, Mizuno & Mineshige 2001).

In contrast to the cold standard model, the slim discs are radiatively inefficient because of both energy advection and photon trapping effects. Consequently, radiation is trapped because of the long photon diffusion time in the vertical direction and advected inwards with the accretion flow (Kato, Fukue & Mineshige 2008 for more details). As a result, the radiation pressure is dominant over gas pressure in slim discs (Mineshige et al. 2000). However similar to the standard disc scenario, supercritical accretion flows emit blackbody-like radiation. The standard model of accretion disc breaks down both in the low-luminosity regimes [optically thin advection dominated accretion flow (ADAFs)] and in high-luminosity regimes (optically thick ADAFs or slim discs).

Some radiation-hydrodynamic (RHD) and radiation-magnetohydrodynamic (RMHD) numerical simulations have shown the existence of outflow in supercritical accretion discs

* E-mail: m.ghasemnezhad@uk.ac.ir (MG); abbassi@um.ac.ir (SA)

(Ohsuga et al. 2005, 2009; Okuda et al. 2005). The RHD simulations of Ohsuga et al. (2005) have demonstrated that the structure of slim discs consists of the disc region and outflow region above and below the disc. Also, Ohsuga et al. (2005) have found that the mass accretion rate does not remain constant with radius and decreases inwards. Blandford & Begelman (1999) proposed the radial dependency of the mass accretion rate as $\dot{M} \propto r^s$ with $0 \leq s \leq 1$ (which the index s is a constant and shows the strength of the wind parameter).

The inward decrease of the inflow accretion rate is related to mass-loss in the form of outflow similar to hot accretion flows. Yang et al. (2014) have found that the outflow can be generated at the surface of the disc because of the radiation pressure force and convection instability when the viscous parameter α is large. But for the small viscous parameter, the slim discs tend to be convectively stable, and the radiation pressure force is the dominant parameter for the generation of outflow. The radiatively driven outflow has been extensively considered by many researchers (e.g. Bisnovatyi-Kogan & Blinnikov 1977; Watarai & Fukue 1999).

The magnetic field plays a crucial role in the dynamical structure and the observational properties of accretion disc. Kaburaki (2000), Abbassi, Ghanbari & Ghasemnezhad (2010), Ghasemnezhad, Khajavi & Abbassi (2012), Samadi, Abbassi & Khajavi (2014), Ghasemnezhad & Abbassi (2016), Ghasemnezhad & Abbassi (2016) and Samadi & Abbassi (2016) have studied the effect of magnetic field on hot accretion flow (ADAF) in recent years. But the magnetized slim disc model has been less studied. Ghasemnezhad, Khajavi & Abbassi (2013) have studied the observational properties of the magnetized slim discs without a wind parameter in two cases such as LMC X-3 and narrow-line Seyfert 1 galaxies.

So the importance and presence of magnetic field in the accretion discs are generally accepted. The magnetic field has several effects such as the formation of the wind/jet (Yuan et al. 2015), the convective stability of accretion flow (Narayan et al. 2012; Yuan, Bu & Wu 2012) and the transfer of angular momentum by an magneto rotational instability (MRI) process in the accretion flow (Balbus & Hawley 1998) on the dynamical and observational appearance of the discs.

So the large-scale ordered magnetic field is another mechanism to produce an outflow in both cold and hot accretion flows. But the magnetic field as the origin of outflow in the hot accretion flow is more important than cold accretion discs. Three-dimensional RMHD simulations by Ohsuga (2009) revealed that the slim disc model is supported by radiation pressure, which is dominant over the gas and magnetic pressures. The magnetic pressure is two times as large as the gas pressure. This simulation has shown that the toroidal component of magnetic field is dominant in the disc inner region, and near the pole, the poloidal component of magnetic field in the vertical direction (along the jet axis) is dominant. So it is important to study the effect of magnetic field on the structure of supercritical accretion flows.

The properties of self-similar solutions for the slim disc are similar to ADAFs and have been pointed out by Fukue (2000). Furthermore, the first self-similar solution for a magnetized ADAF has been presented by Akizuki & Fukue (2006), which is able to reproduce general properties of slim discs. Zahra Zeraatgari, Abbassi & Mosallanezhad (2016) studied the 1.5-dimensional self-similar inflow–outflow equations of supercritical accretion flows with an outflow in the absence of the magnetic field. They have followed the method of Bu, Yuan & Xie (2009) and Xie & Yuan (2008) to study the effects of outflow by considering

the interchange of mass, radial/angular momentum and energy between inflow and outflow. In this paper, we develop Zahra Zeraatgari et al. (2016) solutions by considering the effects of large-scale ordered magnetic field in the 1.5-dimensional inflow–outflow equations.

The hypothesis of the model and relevant equations are developed in Section 2. Self-similar solutions are presented in Section 3. We show the result in Section 4.

2 BASIC EQUATIONS

In this paper, we study the effects of large-scale magnetic field on the structure of supercritical accretion flows with the existence of an outflow by using the method presented by Bu et al. (2009) and Xie & Yuan (2008). In the cylindrical coordinates (r, φ, z) , we write the 1.5-dimensional, steady-state ($\frac{\partial}{\partial t} = 0$) and axisymmetric ($\frac{\partial}{\partial \varphi} = 0$) inflow–outflow equations using the self-similar approach. A height-integrated version of MHD equations (the continuity, the momentum and energy equations) has been adopted, instead of using the two-dimensional equations (e.g. the equations written in the 1.5-dimensional description). Also, we use the Newtonian gravity in the radial direction and neglect the self-gravity of the discs and the general relativistic effects for simplicity. We consider both the z and φ components of the large-scale magnetic field (B_z, B_φ). We do not consider the radial component of magnetic field (B_r), as we noted in the introduction. We investigate the contributions of the two components of magnetic field to removing angular momentum. Also, outflows can contribute to removing the angular momentum, mass and energy from the disc. We suppose the α -prescription for the turbulent viscosity in the rotating gas in the accretion flow.

The MHD equations are as follows (Bu et al. 2009):

$$\frac{d\rho}{dt} + \rho \nabla \cdot \mathbf{v} = 0, \quad (1)$$

$$\frac{d\mathbf{v}}{dt} = -\frac{\nabla p}{\rho} - \nabla \psi + \frac{1}{c} \frac{\mathbf{J} \times \mathbf{B}}{\rho} + \frac{\nabla \times \mathbf{T}}{\rho}, \quad (2)$$

$$\nabla \times \mathbf{B} = \frac{4\pi}{c} \mathbf{J}, \quad (3)$$

$$\nabla \cdot \mathbf{B} = 0. \quad (4)$$

The induction equation of the magnetic field is

$$\frac{\partial \mathbf{B}}{\partial t} = \nabla \times \left(\mathbf{v} \times \mathbf{B} - \frac{4\pi}{c} \eta \mathbf{J} \right). \quad (5)$$

The energy equation for the supercritical accretion flows is

$$Q_{\text{vis}}^+ = Q_{\text{adv}}^- + Q_{\text{rad}}^-, \quad (6)$$

where Q_{adv}^- is the advective cooling written as follows:

$$Q_{\text{adv}}^- = \rho \left(\frac{de}{dt} - \frac{p}{\rho^2} \frac{d\rho}{dt} \right). \quad (7)$$

In the above equations, ρ , \mathbf{v} , p , e , \mathbf{B} , η , \mathbf{T} , ψ , Q_{vis}^+ and Q_{rad}^- denote the density, velocity, total pressure ($p = p_{\text{gas}} + p_{\text{radiation}} + p_{\text{magnetic}}$), gas internal energy ($e = \frac{c_s^2}{\gamma - 1}$, where γ is the specific heat ratio and $c_s^2 = \frac{p}{\rho}$ is the sound speed), magnetic field, magnetic diffusivity, viscous tensor, Newtonian gravitational potential ($\psi = -GM/r$), viscous heating and radiative cooling, respectively. We consider only the azimuthal component of viscous stress tensor as $T = T_{r\varphi} = \rho \nu r \frac{\partial(v_\varphi/r)}{\partial r}$, where ν is the kinematic viscosity. Also, the viscous heating is given as $Q_{\text{vis}}^+ = T_{r\varphi} r \frac{\partial(v_\varphi/r)}{\partial r}$ (Bu et al. 2009; Zahra

Zeraatgari et al. 2016). We have followed the assumptions of Lovelace, Romanova & Newman (1994), Hirose et al. (2004) and Bu et al. (2009) for studying the large-scale magnetic field. We consider the two components of magnetic field, B_z and B_ϕ , in the form of an even function of z and an odd function of z , respectively. Also, the vertical gradient of B_z is neglected. Hirose et al. (2004) have studied numerically the magnetic field topologies in different flow regions, include that of the main disc body, the inner torous and plunging regions, the corona envelope and the funnel part. The numerical MHD simulations carried out by Hirose et al. (2004) have shown that the magnetic field includes two components: the large-scale component and the small-scale component (turbulent component). According to these simulations, the effects of turbulence and the differential rotation control the magnetic field geometry in the main body of the disc. The former bends the field line in all directions, and the latter changes the radial field line into a toroidal field line. So the magnetic field configuration of the main disc body is a tangled toroidal field and a turbulent field. In the plunging and inner regions, the flow changes from a turbulence-dominated inflow to a spiralling inflow. Also in the corona, the magnetic field is purely toroidal without tangles. The large-scale poloidal magnetic field exists only in the funnel part. Therefore, the toroidal magnetic field governs the main body of the flow and its inner parts, while the funnel part is governed by the poloidal magnetic field (which is mostly in the vertical direction z). Thus, we consider two components of large-scale magnetic field, B_z and B_ϕ , and we suppose that $B_r = 0$. We used the α -prescription for the turbulent viscosity that consists of all effects of the small-scale (turbulence) component of magnetic field. In this paper, we consider the even z - symmetry field ($B_\phi(r, z) = -B_\phi(r, -z)$, $B_z(r, z) = +B_z(r, -z)$), and B_z is in the form of an even function of z . We can write the magnetic field as follows:

$$\mathbf{B} = B_p(r, z) + B_\phi(r, z)\hat{\phi}, \quad (8)$$

where B_p and B_ϕ are the poloidal and toroidal magnetic field components. From equation (4), we can express that $\Delta B_z = \frac{H}{r}(B_r)_H$, and by assuming two conditions as $\frac{H}{r} \leq 1$ and $(B_r)_H \leq B_z$, it follows that $\Delta B_z \ll B_z$, that is, we have neglected the variations of B_z with z in the disc. So we have followed the following assumptions:

$$B_r = 0, \quad (9)$$

$$B_\phi = B_0 \frac{z}{H}, \quad \rightarrow B_{\phi, z=H} = -B_{\phi, z=-H}, \quad (10)$$

where H is the half thickness of the accretion disc and B_0 is given by $B_0 = B_{\phi, z=H}$. Also, equation (4) is satisfied by these assumptions. Xie & Yuan (2008) showed that the accretion flow has two parts: inflow and outflow. They have supposed that the vertical velocity for inflow is $v_z = 0$ (i.e. there is a hydrostatic balance in the vertical direction) and the outflow starts from the surface of inflow ($z = H$) with velocity given by $v_{z, w}$, $v_{r, w}$, $v_{\phi, w}$. Therefore, on the surface of the disc, there is discontinuity between outflow and inflow. We have considered the MHD equations that consist of a coupling between the outflow and inflow in the presence of the large-scale magnetic field (Xie & Yuan 2008; Bu et al. 2009). By integrating the equation of conservation of mass in the vertical direction and by defining the mass accretion rate as $\dot{M}(r) = -2\pi r v_r \rho$ and the density ratio of outflow and inflow (η_1) as $\eta_1 = \frac{\rho_w}{\rho} \cong 0.71$ (Xie & Yuan 2008), the continuity equation gives

$$\frac{d\dot{M}(r)}{dr} = \eta_1 4\pi r \rho v_{z, w}. \quad (11)$$

The equations of the conservation of radial, angular and vertical momentum are as follows:

$$\begin{aligned} v_r \frac{dv_r}{dr} + \frac{1}{2\pi r \Sigma} \frac{d\dot{M}(r)}{dr} (v_{r, w} - v_r) &= \frac{v_\phi^2}{r} - \frac{GM}{r^2} \\ &- \frac{1}{\Sigma} \frac{d(\Pi)}{dr} - \frac{1}{4\pi \Sigma} \left[\frac{d}{dr} (H B_z^2) + \frac{1}{3} \frac{d}{dr} (H B_0^2) + \frac{2}{3} \frac{B_0^2}{r} H \right], \quad (12) \end{aligned}$$

$$\begin{aligned} \frac{\Sigma v_r}{r} \frac{d(rv_\phi)}{dr} + \frac{1}{2\pi r} \frac{d\dot{M}(r)}{dr} (v_{\phi, w} - v_\phi) &= \frac{1}{r^2} \frac{d(r^3 v \Sigma \frac{d\Omega}{dr})}{dr} \\ &- \frac{1}{2\pi} B_z B_0, \quad (13) \end{aligned}$$

$$\frac{GM}{r^3} = (1 + \beta_1) c_s^2, \quad (14)$$

where $\Sigma \equiv \int \rho dz$ is the vertically integrated density and $\Pi = \int p dz$ is the vertically integrated pressure. By assuming a dominance of the radiation pressure in supercritical accretion discs, we can write the height-integrated pressure $\Pi = \Sigma c_s^2 = \Pi_{\text{radiation}}$. We neglect the gas pressure. All variables have their own usual meanings, such as v_r , v_ϕ , Ω and G denote the radial speed, the rotational speed, the angular speed of inflow and the gravitational constant, respectively. Also, we use the α -prescription for the viscosity parameter as $\nu = \alpha c_s H$. Apparently, it is almost impossible to solve the equations directly. We therefore, following Xie & Yuan (2008), introduce the parameters ζ_1 and ζ_2 to evaluate the radial and angular velocities of outflow in terms of inflow: $v_{r, w} = \zeta_1 v_r$, $v_{\phi, w} = \zeta_2 v_\phi$.

The ratio of magnetic pressure to radiation pressure is assumed as

$$\beta_1 = \frac{(B_{\phi, z=H})^2 / 8\pi}{\rho c_s^2}, \quad (15)$$

$$\beta_2 = \frac{(B_{z, z=H})^2 / 8\pi}{\rho c_s^2}. \quad (16)$$

Three-dimensional RMHD simulations by Ohsuga (2009) revealed that in the slim disc model the magnetic pressure is smaller than the radiation pressure. So the values of β_1 and β_2 are in the range $\beta_1, \beta_2 < 1$.

The energy equation is as follows:

$$\begin{aligned} \frac{\Sigma v_r}{\gamma - 1} \frac{dc_s^2}{dr} - 2H c_s^2 v_r \frac{d\rho}{dr} + \frac{1}{2\pi r} \frac{d\dot{M}(r)}{dr} (\epsilon_w - \epsilon) \\ = \Sigma \alpha c_s H r^2 \left(\frac{d\Omega}{dr} \right)^2 - \frac{8\Pi c}{k_{\text{es}} \Sigma H}, \quad (17) \end{aligned}$$

where $\epsilon_w = \zeta_3 \epsilon$ (Bu et al. 2009) is the specific internal energy of the outflow. The third term on the left-hand side of equation (27) represents the exchange of internal energy between the inflow and outflow. When $\zeta_3 > 1$, the outflow is the extra cooling rate for the inflow, and when $\zeta_3 < 1$, the outflow is the extra heating rate for the inflow.

The last term of the energy equation is related to radiative cooling rate, which is important in supercritical accretion discs. As mentioned in the introduction, the optically thick ADAFs are supported by radiation pressure. The radiative cooling rate can be written as $Q_{\text{rad}}^- = \frac{8acT_0^4}{3k\rho H} \cong \frac{8\Pi c}{k_{\text{es}} \Sigma H}$, where a and T_0 are the radiation constant and the disc temperature on the equatorial plane. The electron opacity scattering is considered only for the opacity $\bar{k} = k_{\text{es}}$, for simplicity.

The induction equation (5) is the field-escaping/creating rate due to magnetic instability or the dynamo effect. For the steady-state accretion flow, the advection rate of the two components of the magnetic flux should be constant.

3 SELF-SIMILAR SOLUTIONS

The self-similar method is a dimensional analysis and scaling law and is very useful for solving the above equations. Following Bu et al. (2009), self-similarity in the radial direction is supposed:

$$\Sigma = \Sigma_0 \left(\frac{r}{r_{\text{out}}} \right)^s. \quad (18)$$

Akizuki & Fukue (2006) have first introduced this type of solution ($\Sigma \propto r^s$).

$$v_r(r) = -c_1 \alpha \sqrt{\frac{GM}{r_{\text{out}}}} \left(\frac{r}{r_{\text{out}}} \right)^{-\frac{1}{2}}, \quad (19)$$

$$V_\varphi(r) = r\Omega(r) = c_2 \sqrt{\frac{GM}{r_{\text{out}}}} \left(\frac{r}{r_{\text{out}}} \right)^{-\frac{1}{2}}, \quad (20)$$

$$c_s^2 = c_3 \frac{GM}{r_{\text{out}}} \left(\frac{r}{r_{\text{out}}} \right)^{-1}. \quad (21)$$

The accretion rate decreases inwards as

$$\dot{M}(r) = \dot{M}(r_{\text{out}}) \left(\frac{r}{r_{\text{out}}} \right)^{s+\frac{1}{2}} = 2\pi c_1 \alpha \Sigma_0 \sqrt{GM} r_{\text{out}}^{\frac{1}{2}} \left(\frac{r}{r_{\text{out}}} \right)^{s+\frac{1}{2}}, \quad (22)$$

$$\dot{M}(r) = 2\pi c_1 \alpha \Sigma_0 \sqrt{GM} r_{\text{out}}^{\frac{1}{2}} \left(\frac{r}{r_m} \right)^{s+\frac{1}{2}}, \quad (23)$$

where $\dot{M}(r_{\text{out}})$ and Σ_0 are the mass inflow rate at the outer boundary (r_{out}) and the surface density at the outer boundary. Akizuki & Fukue (2006) have shown that there is some restriction in the parameter s . When the parameter $s = -\frac{1}{2}$, there is no mass-loss/wind, but the self-similar model with an outflow could exist only in the case of $s > -\frac{1}{2}$. (We will show that the presence of radiation pressure in the supercritical accretion disc causes that the parameter s was restricted to $s = \frac{1}{2}$.) Also Akizuki & Fukue (2006) have found that for $s = 2$, the creation and escape of magnetic field balance each other.

By substituting the above self-similar solutions into the dynamical equations of the system, we obtain the following system of dimensionless equations, to be solved for c_1 , c_2 and c_3 :

$$-\frac{1}{2}c_1^2\alpha^2 - \left(s + \frac{1}{2}\right)(\zeta_1 - 1)c_1^2\alpha^2 = c_2^2 - 1 - (s - 1)c_3 - \beta_2(s - 1)c_3 - \frac{1}{3}\beta_1(s - 1)c_3 - \frac{2}{3}\beta_1c_3, \quad (24)$$

$$\alpha c_1 c_2 - 2\alpha \left(s + \frac{1}{2}\right)(\zeta_2 - 1)c_1 c_2 = 3\alpha c_3 c_2 (s + 1) \sqrt{1 + \beta_1} + 4\sqrt{\frac{c_3 \beta_1 \beta_2}{1 + \beta_1}}, \quad (25)$$

$$\frac{H}{r} = \sqrt{(1 + \beta_1)c_3}, \quad (26)$$

$$\frac{1}{\gamma - 1} + (s - 1) + \frac{(s + \frac{1}{2})(\zeta_3 - 1)}{\gamma - 1} = \frac{9}{4} \frac{c_2^2}{c_1} \sqrt{1 + \beta_1} - \frac{8}{\dot{m} \sqrt{(1 + \beta_1)c_3}} \left(\frac{r_{\text{out}}}{r_s} \right) \left(\frac{r}{r_{\text{out}}} \right)^{-s+\frac{1}{2}}. \quad (27)$$

For the last term of equation (27), we use a few definitions such as

$$\dot{m} = \frac{\dot{M}_{\text{out}}}{\dot{M}_{\text{crit}}}, \quad (28)$$

$$\dot{M}_{\text{out}} = 2\pi\alpha c_1 \Sigma_0 r_{\text{out}}^{\frac{1}{2}}, \quad (29)$$

$$\dot{M}_{\text{crit}} = \frac{L_E}{c^2} = \frac{4\pi GM}{ck_{\text{es}}}, \quad (30)$$

$$r_s = \frac{2GM}{c^2}, \quad (31)$$

where r_s , L_E and c are the Schwarzschild radius, Eddington luminosity and speed of light, respectively. The last term in equation (27), which is the radiative cooling rate, has the same radial dependency on advection cooling and viscously heating rates when $s = \frac{1}{2}$ (Zahra Zeraatgari et al. 2016).

The second term on the left-hand side of equation (25) is angular momentum transfer between inflow and outflow (the angular momentum taken away from the inflow by the outflow when $\zeta_2 > 1$ or deposited into the inflow by the outflow if $\zeta_2 < 1$). Also, on the right-hand side of this equation, we have the angular momentum transfer by turbulent viscosity and the large-scale magnetic field, respectively.

On the right-hand side of equation (25), we have two terms representing angular momentum transportation due to turbulent viscosity and large-scale magnetic field, respectively. Following Bu et al. (2009), we defining a new parameter c_4 , which is the ratio of these two terms:

$$c_4 = \frac{3\alpha c_3 c_2 (s + 1) \sqrt{1 + \beta_1}}{4\sqrt{\frac{c_3 \beta_1 \beta_2}{1 + \beta_1}}}. \quad (32)$$

For given values of α , \dot{m} , ζ_1 , ζ_2 , ζ_3 , β_1 and β_2 , these equations (c_1 , c_2 , c_3 and c_4) can be worked out numerically. Our results reduce to the results of Zahra Zeraatgari et al. (2016) without large-scale magnetic field.

4 RESULTS

4.1 Dynamical structure

We are interested in studying the effects of large-scale magnetic field (β_1 , β_2) on the structure of accretion disc. In all figures, following Zahra Zeraatgari et al. (2016), we adopt the constant values of $\alpha = 0.1$, $r_{\text{out}} = 100r_s$, $s = \frac{1}{2}$, $\gamma = \frac{4}{3}$ and $M = 10^6 M_\odot$. In all the six panels of Figs 1 and 2, we investigate the effects of large-scale magnetic field [azimuthal (β_1) and vertical (β_2) components of magnetic field] on the radial velocity (c_1), rotational velocity (c_2) and relative thickness ($\frac{H}{r}$) of accretion flow. Figs 1 and 2 show the coefficients c_1 , c_2 and $\frac{H}{r}$ in terms of the mass inflow rate \dot{m} at the outer boundary for different values of magnetic parameters $\beta_{1,2}$ ($\beta_{1,2} = 0.1, 0.2, 0.3$). As we can easily see from the two figures, for larger values of the mass inflow rate \dot{m} , the radial velocity and relative thickness of the disc increase, but the rotational velocity decreases. It is in good agreement with Zahra Zeraatgari et al. (2016). Both radial and rotational velocities are sub-Keplerian. By increasing the mass accretion, more energy will be released and, consequently, the disc becomes thicker. On the other hand, the radiation pressure dominated region extends from the inner region of the disc to the outer region. Furthermore, when the azimuthal magnetic field $B_\varphi(\beta_1)$ becomes stronger in Fig. 1, the radial velocity, the rotational velocity and thickness of the inflow increase. A magnetized disc must rotate faster and accrete more inwards than when there is non-magnetic field present because of the effect of magnetic tension force [the last term on the right-hand side of equation (24) is the magnetic stress force ($-\frac{2}{3}\beta_1 c_3$)]. As can be seen,

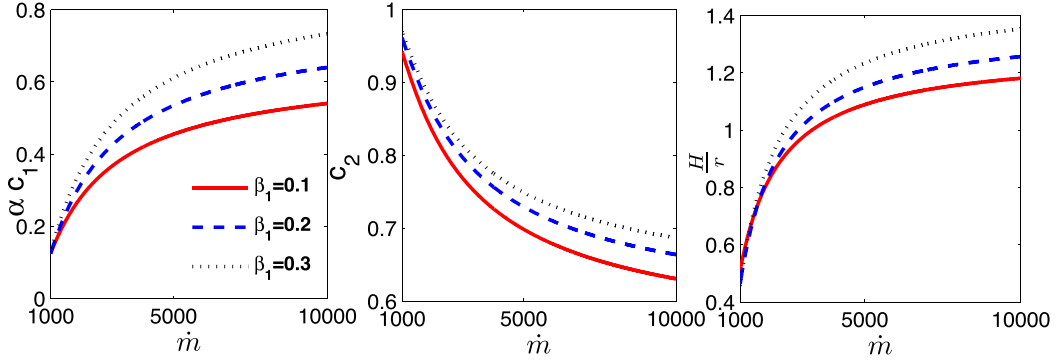


Figure 1. Numerical coefficients c_1 and c_2 and $\frac{H}{r}$ as a function of mass inflow rate \dot{m} for several values of β_1 (the toroidal component of magnetic field). For all panels, we use $s = 0.5$, $\gamma = 1.33$, $\alpha = 0.1$, $\zeta_{1,2} = 0.5$, $r_{\text{out}} = 100$, $\zeta_3 = 0.2$ and $\beta_2 = 0.05$.

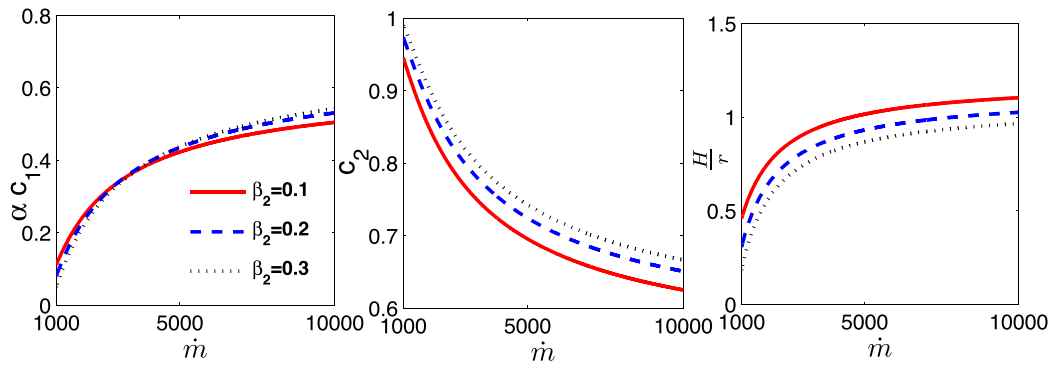


Figure 2. Numerical coefficients c_1 and c_2 and $\frac{H}{r}$ as a function of mass inflow rate \dot{m} for several values of β_2 (the vertical component of magnetic field). For all panels, we use $s = 0.5$, $\gamma = 1.33$, $\alpha = 0.1$, $\zeta_{1,2} = 0.5$, $r_{\text{out}} = 100$, $\zeta_3 = 0.2$ and $\beta_1 = 0.05$.

by increasing the toroidal component of magnetic field in the main body of the disc, the disc becomes thicker (see equation 26). In Fig. 2, the vertical component of magnetic field changes from 0.1, 0.2 and 0.3. Similar to Fig. 1, the radial and azimuthal velocities have an increasing trend with respect to the vertical component of magnetic field β_2 , while the disc becomes thinner by increasing the vertical component of magnetic field in the high accretion mass. Bu et al. (2009) have shown that in the ADAF model, the large-scale magnetic field and outflow cause the reduction of the sound speed of the disc and then the reduction of the thickness of the disc. But, we have shown numerically that the two components of magnetic field have opposite effects on the thickness of the disc.

The effects of large-scale magnetic field components and outflow parameters on c_4 have been plotted in Fig. 3. As we can see in equation (32), if $c_4 < 1$, the dominant mechanism in angular momentum transport will be the large-scale magnetic field. As the large-scale magnetic field in $\beta_{1,2}$ increases, it is obvious that the contributions of turbulent viscosity to transportation of angular momentum decrease, which is in good agreement with Bu et al. (2009). This is because the large-scale magnetic field leads to the inflow gaining more angular momentum. In Fig. 3, it is clear that when $\beta_{1,2} < 0.1$, the effects of large-scale magnetic field are almost negligible, while for $\beta_{1,2} > 0.1$, the parameter c_4 is below unity and so this leads to decreasing the turbulent viscosity contribution in angular momentum transportation. Also in Fig. 3, we have represented the effect of the angular momentum and the specific internal energy of outflow $\zeta_{2,3}$ on the parameter c_4 . We can see from Fig. 3 that for $\beta_{1,2} < 0.1$,

ζ_2 has a very weak effect on c_4 while ζ_3 has a significant effect on c_4 . Generally, by increasing both $\zeta_{2,3}$, c_4 decreases. These results are consistent with solutions of Bu et al. (2009).

We can calculate the effects of the exchange of energy and momentum between inflow and outflow and magnetic field on the advection parameter (f). Narayan & Yi (1994) introduced the advection parameter as $f = \frac{Q_{\text{vis}}^+ - Q_{\text{rad}}^-}{Q_{\text{vis}}^+} = \frac{Q_{\text{adv}}^-}{Q_{\text{vis}}^+}$. We can write the ratio of advection cooling to viscous heating (f) as follows:

$$f = \frac{\frac{1}{\gamma-1} + (s-1) + \frac{(s+\frac{1}{2})(\zeta_3-1)}{\gamma-1}}{\frac{9}{4} \frac{c_2^2}{c_1} \sqrt{1+\beta_1}}. \quad (33)$$

We have shown the effects of large-scale magnetic field $\beta_{1,2}$ and the angular momentum ζ_2 and specific energy ζ_3 of outflow on the advection parameter f in Fig. 4 (plotting the advection parameter f with respect to \dot{m}). We can see that when the mass inflow rate \dot{m} increases, the advection parameter f increases, and when the specific internal energy of outflow ($\zeta_3 = 0.2, 0.5$ and 0.9) increases, the advection parameter also increases (it is simply understood from equation 33). The second term in the numerator of equation (33) $[(s + \frac{1}{2})(\zeta_3 - 1)]$ is related to interchange of energy between outflow and inflow, and for $\zeta_3 < 1$, it is negative. So when ζ_3 becomes larger, this expression becomes smaller and then the advection parameter increases. As we have mentioned, the outflow can play a role in extra heating when $\zeta_3 < 1$. On the other hand, the advection

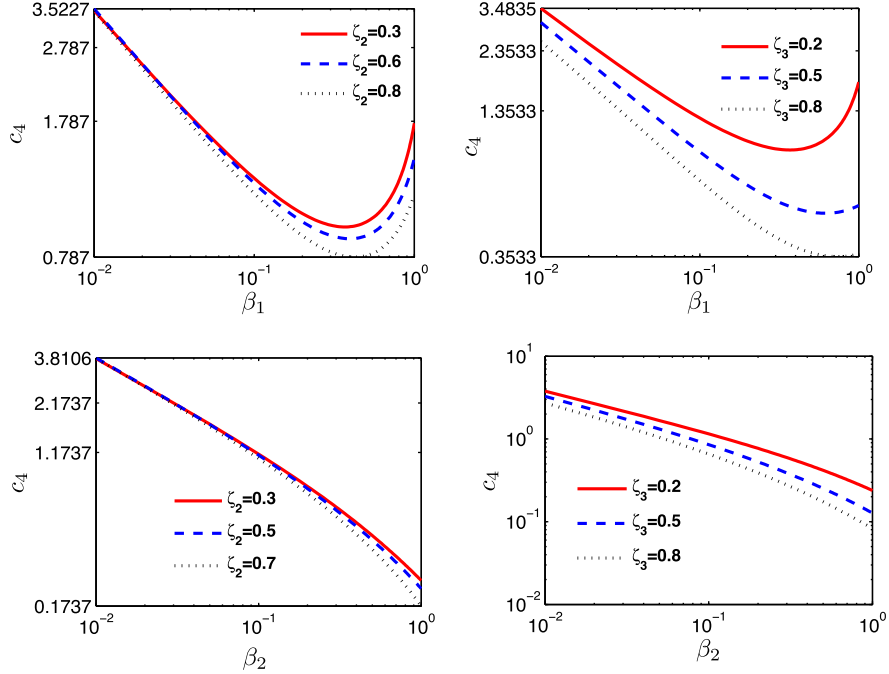


Figure 3. The ratio between angular momentum transport by turbulent viscosity and magnetic field as a function of large-scale magnetic field $\beta_{1,2}$ for several values of $\zeta_{2,3}$. For all panels, we use $s = 0.5$, $\gamma = 1.33$, $\alpha = 0.1$, $\zeta_1 = 0.5$, $r_{\text{out}} = 100$ and $\dot{m} = 3000$. In the upper and bottom panels, we use $\beta_2 = 0.05$ and $\beta_1 = 0.05$, respectively.

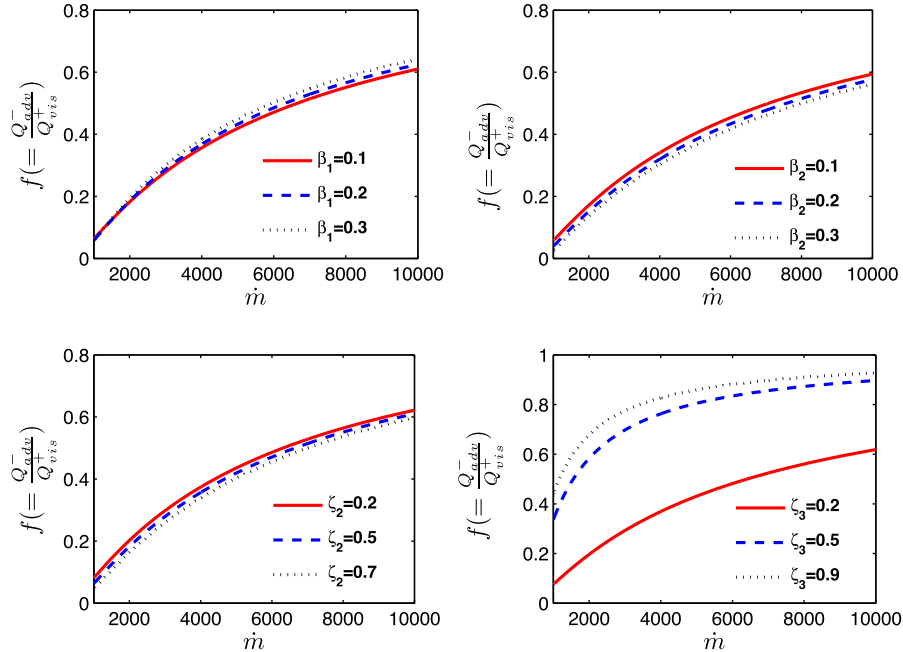


Figure 4. The advection parameter f as a function of mass inflow rate \dot{m} for several values of $\beta_{1,2}$ and $\zeta_{2,3}$. For all panels, we use $s = 0.5$, $\gamma = 1.33$, $\alpha = 0.1$, $\zeta_1 = 0.5$ and $r_{\text{out}} = 100$.

parameter is independent of the components of magnetic field $\beta_{1,2}$ and the angular momentum of outflow ζ_2 .

4.2 The bolometric luminosity

In the slim disc model, the mass accretion rate and the optical depth are very high. So, the radiation generated by an accretion disc can be trapped within the disc, the radiation pressure dominates and the

sound speed is related to radiation pressure. Slim discs radiate away locally like a blackbody radiation. The emergent local flux F is

$$F = \sigma T_{\text{eff}}^4 = \frac{1}{2} Q_{\text{rad}}^- = \frac{16 \sigma T_0^4}{3 \tau} = \frac{4 \Pi c}{k_{\text{es}} \Sigma H}, \quad (34)$$

where σ and $\tau (= \frac{1}{2} k_{\text{es}} \Sigma)$ are the Stefan–Boltzmann constant and the optical depth of the flow, respectively. The factor 2 comes from the fact that the radiation will be radiated from both sides of the

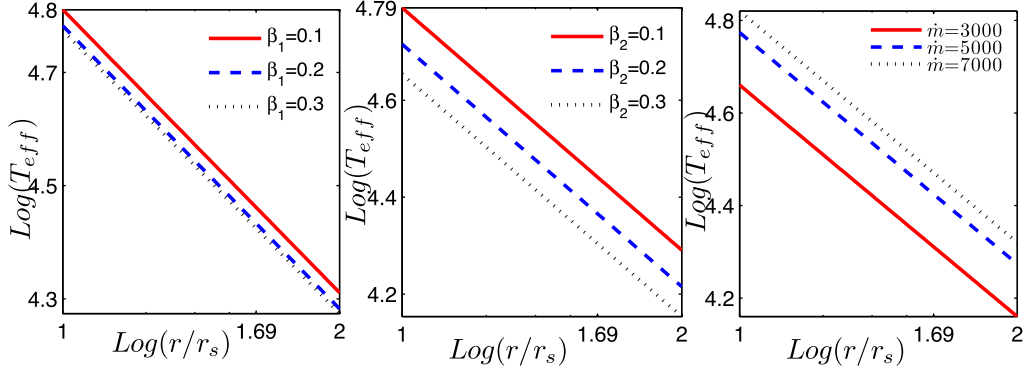


Figure 5. The effective temperature as a function of dimensionless radius r/r_s for several values of $\beta_{1,2}$ and \dot{m} . For all panels, we use $s = 0.5$, $\gamma = 1.33$, $\alpha = 0.1$, $\zeta_{1,2} = 0.5$, $\zeta_3 = 0.2$ and $r_{\text{out}} = 100$. We set $\beta_2 = 0.05$ for the left-hand panel, $\beta_1 = 0.05$ for the middle panel and $\beta_1 = 0.3$, $\beta_2 = 0.05$ for the right-hand panel.

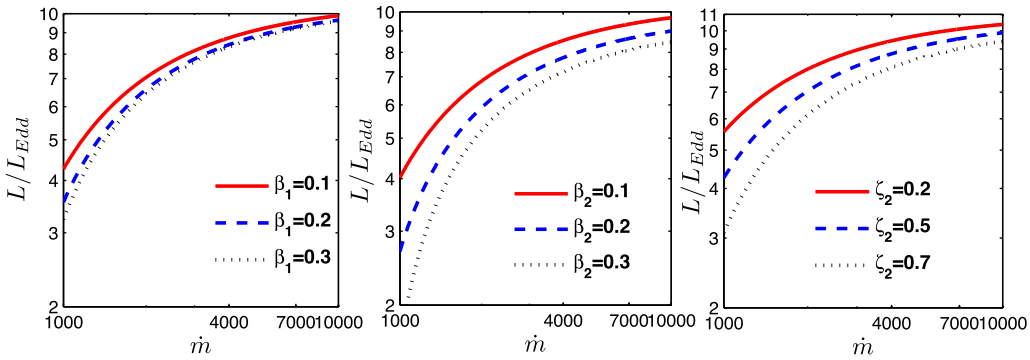


Figure 6. Bolometric luminosity as a function of mass inflow rate \dot{m} for several values of $\beta_{1,2}$ and ζ_2 . For all panels, we use $s = 0.5$, $\gamma = 1.33$, $\alpha = 0.1$, $\zeta_1 = 0.5$, $\zeta_3 = 0.2$ and $r_{\text{out}} = 100$. We set $\beta_2 = 0.05$ and $\zeta_2 = 0.5$ for the left-hand panel, $\beta_1 = 0.05$ and $\zeta_2 = 0.5$ for the middle panel, and $\beta_1 = 0.1$ and $\beta_2 = 0.05$ for the right-hand panel.

disc. So, by using the relation $\frac{\pi}{\Sigma} = c_s^2$ and the self-similar solutions, we can obtain the emergent local flux and surface temperature of the disc as follows:

$$F(r) = \sigma T_{\text{eff}}^4 = \frac{4c}{k_{\text{es}}} \sqrt{\frac{c_3}{1 + \beta_1}} \frac{GM}{r^2}, \quad (35)$$

$$T_{\text{eff}} = \left(\frac{L_E}{\pi\sigma}\right)^{\frac{1}{4}} \left(\frac{c_3}{1 + \beta_1}\right)^{\frac{1}{8}} r^{-\frac{1}{2}}. \quad (36)$$

The self-similar solutions for the flux and effective temperature without magnetic field was first presented by Watarai & Fukue (1999). In comparison with their solutions (without magnetic field), in our solutions the flux and effective temperature depend on the toroidal component of magnetic field β_1 explicitly ($\frac{1}{1 + \beta_1}$) and on the vertical component of magnetic field β_2 through c_3 implicitly. In Fig. 5, the surface temperature is plotted for different amounts of large-scale magnetic field ($\beta_{1,2}$) and mass accretion rates at the outer boundary (\dot{m}) in terms of dimensionless radius ($\frac{r}{r_s}$). It is clear that the surface temperature decreases as $\frac{r}{r_s}$ increases. We can conclude that at larger values of the magnetic field parameters ($\beta_{1,2}$), for a constant radius, the temperature of the flow will decrease. A magnetized disc must rotate faster and accrete more inwards because of the effect of magnetic stress force (or a centripetal force). As a result, the centrifugal force [both the radiation pressure gradient force ($\propto c_3$) and the magnetic pressure gradient force ($\propto c_3$)] decreases in the presence of large-scale magnetic field since the

temperature (c_3) decreases for a wide range of $\beta_{1,2}$. On the other hand, the solution shows that the surface temperature increases as the mass inflow rate at the outer boundary increases, which is in agreement with the solution presented by Watarai et al. (2000).

It is possible to calculate an analytic expression for $L = L(\dot{m})$. We derive the bolometric luminosity of the slim discs for a typical central black hole with $M = 10^6 M_{\odot}$ as follows:

$$L = 2 \int_{r_{\text{in}}=10r_s}^{r_{\text{out}}=100r_s} F(r) 2\pi r dr. \quad (37)$$

The luminosity of the supercritical accretion disc is plotted in Fig. 6, as a function of mass accretion rate for different values of large-scale magnetic field $\beta_{1,2}$ and angular momentum carried by the outflow ζ_2 . The bolometric luminosity of slim discs increases with increasing mass accretion rate \dot{m} . As a result of photon trapping in the supercritical accretion flows, the maximum luminosity of slim discs becomes insensitive to the mass accretion rate when $\dot{m} \gg 1$ ($L/L_E \propto \dot{m}^0 \approx \text{constant}$). The disc luminosity is always kept around the Eddington luminosity if the mass accretion rate greatly exceeds unity. We can easily see that the luminosity of the slim discs decreases with the addition of the two components of magnetic field and the angular momentum carried by the outflow and becomes $L \approx 10L_E$ for larger values of \dot{m} . These results are in good agreement with Zahra Zeraatgari et al. (2016) and with simulations performed by Ohsuga et al. (2005, see fig. 7) and Watarai et al. (2000, see fig. 3).

5 SUMMARY AND CONCLUSION

In this paper, we have investigated the effects of large-scale magnetic field on a supercritical accretion flow in the presence of an outflow. It was assumed that an outflow contributes to loss of mass, angular momentum and thermal energy from accretion discs. By using the method presented by Bu et al. (2009) and Xie & Yuan (2008), we consider the discontinuity between mass, momentum (radial and azimuthal components of momentum) and energy outflow and inflow. Also, simulations have indicated that the large-scale ordered magnetic field exists in the accretion disc and can produce an outflow in both cold and hot accretion flows. RMHD simulations have shown that the azimuthal component of magnetic field is dominant in the main body of the disc and the vertical component of magnetic field is dominant near the pole.

We used the self-similar method for solving the 1.5-dimensional, steady-state ($\frac{\partial}{\partial t} = 0$) and axisymmetric ($\frac{\partial}{\partial \varphi} = 0$) inflow–outflow equations. The self-similar solutions are very useful to improve our understanding of the physics of the accretion discs around a black hole. Also, we ignore the relativistic effects and self-gravity of the disc and use Newtonian gravity in the radial direction. We consider the effect of $B_{\varphi, z}$ on the dynamics of a disc by following Zahra Zeraatgari et al. (2016) in the presence of the effect of wind. Our results reproduce their solutions when the effect of large-order magnetic field is neglected. The disc accretes more and rotates fast in the presence of large-scale magnetic field. Also, we have shown that the two components of magnetic field have the opposite effects on the thickness and the sound speed of the disc. We find that the strong magnetic field decreases the contribution of turbulence viscosity in angular momentum transfer. The solutions indicated that the mass inflow rate and specific energy of outflow have a strong effect on the advection parameter. The outflow is the extra heating rate for the inflow when $\zeta_3 < 1$. We find that by increasing the energy of outflow, the advection parameter increases.

Furthermore, we have examined how the two components of magnetic field affect the luminosity and surface temperature of the supercritical accretion disc. As we have mentioned in the previous section, the effective temperature as well as the bolometric luminosity has a decreasing behaviour in respect to the two components of magnetic field.

In addition, increasing the mass accretion rate increases the temperature and luminosity of the disc, while the luminosity of the disc (L) is insensitive to a mass accretion rate $\dot{m} \gg 1$. We have shown that the maximum luminosity is kept constant and $L \approx 10L_E$, which is in good agreement with calculations done by Watarai et al. (2000) and Ohsuga et al. (2005). Although we have made some simplification and imposed some limitations in order to solve equations numerically, our results show that ordered large-scale magnetic field and outflow can really change the structure of supercritical accretion flow, which means that in any realistic model, these factors should be taken into account. So, self-similar solutions could interpret well the numerical simulations and observational evidence.

ACKNOWLEDGEMENTS

SA acknowledges support from the Department of Astronomy, Cornell University, where a part of this work has been done, for their hospitality during a visit. We also appreciate the referee for his/her thoughtful and constructive comments on an early version of this paper.

REFERENCES

- Abbassi S., Ghanbari J., Ghasemnezhad M., 2010, *MNRAS*, 409, 1113
 Abramowicz M. A., Czerny B., Lasota J. P., Szuszkiewicz E., 1988, *ApJ*, 332, 646
 Akizuki C., Fukue J., 2006, *PASJ*, 58, 469
 Balbus S. A., Hawley J. F., 1998, *Rev. Mod. Phys.*, 70, 1
 Begelman M. C., Meier D. L., 1982, *ApJ*, 253, 873
 Bisnovatyi-Kogan G. S., Blinnikov S. I., 1977, *A&A*, 59, 111
 Blandford R. D., Begelman M. C., 1999, *MNRAS*, 303, L1
 Bu D. F., Yuan F., Xie F. G., 2009, *MNRAS*, 392, 325
 Fukue J., 2000, *PASJ*, 52, 829
 Ghasemnezhad M., Abbassi S., 2016, *Ap&SS*, 361, 372
 Ghasemnezhad M., Abbassi S., 2016, *MNRAS*, 456, 71
 Ghasemnezhad M., Khajavi M., Abbassi S., 2012, *ApJ*, 750, 57
 Ghasemnezhad M., Khajavi M., Abbassi S., 2013, *Ap&SS*, 346, 341
 Hirose S., Krolik J. H., De Villiers J. P., Hawley J. F., 2004, *ApJ*, 606, 1083
 Kaburaki O., 2000, *ApJ*, 660, 1273
 Kato S., Fukue J., Mineshige S., 2008, *Black Hole Accretion Discs*. Kyoto University Press, Kyoto
 Lovelace R. V. E., Romanova M. M., Newman W. I., 1994, *ApJ*, 437, 136
 Mineshige S., Kawaguchi T., Takeuchi M., Hayashida K., 2000, *PASJ*, 52, 499
 Narayan R., Yi I., 1994, *ApJ*, 428, L13
 Narayan R., Sadowski A., Penna R. F., Kulkarni A. K., 2012, *MNRAS*, 426, 3241
 Ohsuga K., ed., 2009, *Proc. IAU Symp. Astrophysics with All-Sky X-Ray Observations*, Vol. 1. Kluwer, Dordrecht, p. 148
 Ohsuga K., Mori M., Nakamoto T., Mineshige S., 2005, *ApJ*, 628, 368
 Ohsuga K., Mineshige S., Mori M., Kato Y., 2009, *PASJ*, 61, L7
 Okuda T., Teresi V., Toscano E., Molteni D., 2005, *MNRAS*, 357, 295
 Samadi M., Abbassi S., 2016, *MNRAS*, 455, 3381
 Samadi M., Abbassi S., Khajavi M., 2014, *MNRAS*, 437, 3124
 Watarai K., Fukue J., 1999, *PASJ*, 51, 725
 Watarai K., Fukue J., Takeuchi M., Mineshige S., 2000, *PASJ*, 52, 133
 Watarai K., Mizuno T., Mineshige S., 2001, *ApJ*, 549, L77
 Xie F. G., Yuan F., 2008, *ApJ*, 681, 499
 Yang X. H., Yuan F., Ohsuga K., Bu D. F., 2014, *ApJ*, 780, 79
 Yuan F., Bu D., Wu M., 2012, *ApJ*, 761, 130
 Yuan F., Gan Z., Narayan R., Sadowski A., Bu D., Bai X. N., 2015, *ApJ*, 804, 101
 Zahra Zeraatgari F., Abbassi S., Mosallanezhad A., 2016, *ApJ*, 823, 98

This paper has been typeset from a $\text{\TeX}/\text{\LaTeX}$ file prepared by the author.